UNIVERSIDADE DE SÃO PAULO

INSTITUTO DE FÍSICA
CAIXA POSTAL 20516
01498 - SÃO PAULO - SP
BRASIL

PUBLICAÇÕES

IFUSP/P-848

COULOMB VERSUS STRONG INTERACTION IN CORRELATED NUCLEON EMISSION

M.E. Bracco, F.S. Navarra and M.C. Nemes
Instituto de Física, Universidade de São Paulo

Maio/1990

COULOMB VERSUS STRONG INTERACTION IN CORRELATED NUCLEON EMISSION

M.E. Bracco, F.S. Navarra and M.C. Nemes
Instituto de Física, Universidade de São Paulo
C.P. 20516, 01498 São Paulo, SP, Brazil

ABSTRACT

We investigate the effect of the Coulomb and strong interaction on double nucleon emission in peripheral heavy ion collisions for incident energies above 1.0 GeV/u. We find that for lower bombarding energies (~ 1.0 GeV/u) the two contributions are well separated and the two processes lead to double nucleon emission in distinct kinetic energy ranges. The effect of the Coulomb interaction rises logarithmically and becomes dominant at increasing bombarding energies (~ 100 GeV/u).

1. INTRODUCTION

In the past decade much effort has been dedicated to the understanding of relativistic heavy ion collisions. Although the main expectation was always to find the QCD plasma, which was supposed to manifest itself in central collisions, there was very interesting physics hidden in peripheral collisions[1]. Among a variety of phenomena, nucleon emission has been also object of investigation. As was pointed out by Feshbach and Zabek[2] at increasing projectile energies double nucleon correlated emission tends to become more important than single nucleon emission because of short range correlations among target nucleons and because of the phonon nature of the target matter excitation.

Recently, Bertulani et al.[3] suggested that in such peripheral reactions the measurement of double nucleon emission cross sections could reveal something important about nuclear structure: the typical length of short range correlations. The main purpose of this paper is to include the Coulomb interaction and investigate how the results of ref. 3 are modified. As we shall see, such contributions are by no means negligible and could be tested experimentally: while the nuclear induced double nucleon emission shows a weak energy dependence, the Coulomb interaction has the typical logarithmic dependence. Therefore it should become dominant for high enough bombarding energies (~ 100 GeV/u). Moreover, the energy of the emitted nucleons could be observed in different ranges for lower bombarding energies (~ 1 GeV/u): Coulomb interaction favors lower kinetic energies of the outcoming nucleons. The situation of course changes as the bombarding energy is increased.

We have dedicated special effort to derive analytical results in order to bring about the essential physics of the process. This was possible by confining ourselves to nucleon emission along the incident beam axis (as done in ref. 3). Extensions of our results for other combinations of projectile and target and/or bombarding energies are therefore immediate.

In what follows we make use of the theory developed in ref. 3 and include the Coulomb interaction. In sec. 2 we describe the formalism and for the sake of completeness repeat the main steps presented in ref. 3. In sec. 3 we show our numerical results and compare them with the previously obtained by Bertulani et al. Finally sec. 4 is reserved for comments and conclusions.

2. FORMALISM

2a. DEFINITIONS

The relativistic peripheral collision, which we will be talking about, is depicted in Fig. 1. To a first order perturbation approximation the amplitude for this process can be written as

$$a_{fi}(b) = \frac{1}{i\hbar}\int_{-\infty}^{+\infty} dt\, e^{i\omega t}\int d^3r_1 \int d^3r_2\, \psi_f^*(\vec r_1,\vec r_2)\Big[V_s(r_1,t) + V_s(r_2,t)$$

$$+ V_c(r_1,t) + V_c(r_2,t)\Big]\, \psi_i(\vec r_1,\vec r_2) \qquad (1)$$

where $V_c(r_i,t)$ and $V_s(r_i,t)$ represent the Coulomb and strong potential respectively, acting between the projectile and the i^{th} nucleon and $\hbar\omega = E_f - E_i = \varepsilon_1 + \varepsilon_2 +$ binding energy of the pair (= 16 MeV). ε_1 and ε_2 are the kinetic energies of nucleons 1 and 2. The choice of the nucleonic pair wave function will be kept the same as in ref. 3 (although the objection should be made, that they are not orthonormal to each other. This effect has been studied by L. Barz et al.[4] with the conclusion that the results are not very much altered for most of the double differential cross section calculated in (3)) namely:

$$\psi_f(\vec r_1,\vec r_2) = e^{i\vec k_1\vec r_1}\, e^{i\vec k_2\vec r_2} \qquad (2)$$

where $\vec k_i$ $(i = 1, 2)$ are the wave vectors of the emitted nucleons. The initial wave function is given by

$$\psi_i(\vec r_1,\vec r_2) = N \exp\left\{-\frac{r_1^2}{2\alpha_T^2}\right\} \exp\left\{-\frac{r_2^2}{2\alpha_T^2}\right\} \left[1 - \exp\left\{-\frac{|\vec r_1-\vec r_2|^2}{r_c^2}\right\}\right] \qquad (3)$$

where N is the appropriate normalization constant, r_c the correlation range and α_T the Gaussian width related to the radius and diffuseness of the target density: $\alpha_T = 2\sqrt{aR_T}$.

In order to simplify the calculations the Gaussian approximation[5] for the strong potential has been adopted in ref. (3) and also here for the sake of comparison. Accordingly, the potential created by the projectile centered at the position (X,Y,Z), with $b = \sqrt{X^2+Y^2}$, and $Z = vt$, is given by

$$V_s(\vec r_i,t) = \gamma V_g \exp\left\{-\frac{(X-x_i)^2}{\alpha_p^2}\right\} \exp\left\{-\frac{(Y-y_i)^2}{\alpha_p^2}\right\} \exp\left\{-\gamma^2\frac{(vt-z_i)^2}{\alpha_p^2}\right\} \qquad (4)$$

where $\gamma = (1-v^2/c^2)^{-1/2}$ is the standard relativistic factor introduced here to take into account the Lorentz contraction of the nucleonic density of the projectile which generates the potential. The strength V_g and the range parameter α_p are

$$V_g = \frac{V_0}{2} \exp\left\{\frac{R_p}{2a}\right\} \qquad \alpha_p = 2\sqrt{aR_p} \qquad (5)$$

where R_p is the radius of the projectile.

The Coulomb potential reads

$$V_c(\vec{r}_i,t) = \frac{Z_p\ e\ \gamma}{\sqrt{(x_i-X)^2+(y_i-Y)^2+\gamma^2(z_i-vt)^2}} . \tag{6}$$

As can be seen from the above equation, the Coulomb interaction is taken to be that of a point like projectile, which follows a straight line trajectory. In ref. 6 it is shown that the evaluation of Coulomb excitation processes, where the projectile remains in its ground state in a field theoretical formulation, considering both nuclei as extended objects leads to the same quantitative result as given by eq. (6).

We shall now proceed the evaluation of (1), which can be decomposed into its Coulomb and nuclear contributions,

$$a_{fi} = \frac{Z_T}{\sqrt{2}}(a_{c_1}+a_{c_2}) - \frac{A_T}{\sqrt{2}}(a_{s_1}+a_{s_2}) \tag{7}$$

where s and c stand for Coulomb and strong respectively. The constant factors multiplying the amplitudes mean that the purely strong part of the cross section is proportional to $A_T^2/2$ (the number of nucleon pairs in the target) and the purely Coulomb part of it is proportional to $Z_T^2/2$ (the number of charged nucleon pairs in the target).

We first evaluate a_{s_1} and a_{c_1}. a_{s_2} and a_{c_2} are obtained by just replacing everywhere the index 1 by 2.

2b. THE STRONG PART OF THE AMPLITUDE a_{s_1}

In this section we shall simply sketch the main steps which led to the analytical expression for the strong interaction, since this has been done in ref. 3. Our purpose here is the discussion of the energy dependence of the strong interaction cross section.

Using the wave functions (2) and (3) and the potential (4) in the definition of the amplitude (1) one gets

$$a_{s_1} = \frac{1}{i\hbar}\int_{-\infty}^{+\infty} dt\, e^{i\omega t} \int d^3r_1 \int d^3r_2\, e^{-i\vec{k}_1\vec{r}_1}\, e^{-i\vec{k}_2\vec{r}_2}\, \gamma V_g \exp\left\{-\frac{(X-x_1)^2}{\alpha_p^2}\right\} \exp\left\{-\frac{(Y-y_1)^2}{\alpha_p^2}\right\}$$

$$\times \exp\left\{-\frac{\gamma^2}{\alpha_p^2}(vt-z_1)^2\right\} N \exp\left\{-\frac{r_1^2}{2\alpha_T^2}\right\} \exp\left\{-\frac{r_2^2}{2\alpha_T^2}\right\} \left[1-\exp\left\{-\frac{|\vec{r}_1-\vec{r}_2|^2}{r_c^2}\right\}\right] .$$

The integration over time can be easily performed

$$\int_{-\infty}^{+\infty} dt \exp\left\{i\omega t - \frac{\gamma^2}{\alpha_p^2}(vt-z_1)^2\right\} = \alpha_p \frac{\sqrt{\pi}}{\gamma v} \exp\left\{-\frac{\alpha_p^2}{4\gamma^2 v^2}\omega^2\right\} \exp\left\{i\frac{\omega}{v}z_1\right\}$$

and the amplitude can be written as an integral in cartesian coordinates

$$a_{s_1} = \frac{V_g\ N\ \alpha_p\ \sqrt{\pi}}{i\hbar v} \exp\left\{-\frac{\alpha_p^2\ \omega^2}{4\gamma^2 v^2}\right\} \int dx_1 \int dx_2 \int dy_1 \int dy_2 \int dz_1 \int dz_2$$

$$\times \exp\left\{-i\left[k_{1x}x_1 + k_{1y}y_1 + k_{1z}z_1 + k_{2x}x_2 + k_{2y}y_2 + k_{2z}z_2\right]\right\}$$

$$\times \exp\left\{-\frac{(X-x_1)^2}{\alpha_p^2} - \frac{(Y-y_1)^2}{\alpha_p^2} + i\frac{\omega}{v}z_1\right\} \exp\left\{-\frac{(x_1^2+y_1^2+z_1^2+x_2^2+y_2^2+z_2^2)}{2\alpha_T^2}\right\}$$

$$\times \left[1-\exp\left\{-\frac{(x_1-x_2)^2}{r_c^2} - \frac{(y_1-y_2)^2}{r_c^2} - \frac{(z_1-z_2)^2}{r_c^2}\right\}\right] . \tag{8}$$

We clearly see that the above amplitude is a sum of two 6–fold integrals. The first one comes from the constant term inside the brackets in the last line and contains no information about correlations. These are in the second term (the exponential), which mixes coordinates of particles 1 and 2. As can be seen from (8) all integrals are gaussian and in the limit $r_c \ll \alpha_T, \alpha_p$ an analytical expression can be obtained for eq. (8) (details in ref. 3). We get

$$a_s = i\,B\,\exp\left\{-\frac{b^2}{4a(R_p+R_T)} - i\,\frac{R_T}{(R_p+R_T)}(k_{1y}+k_{2y})\,b\right\}\left[\exp\left\{-\frac{r_c^2}{4}(k_{2x}^2+k_{2y}^2+k_{2z}^2)\right\}\right.$$

$$\left.+\exp\left\{-\frac{r_c^2}{4}(k_{1x}^2+k_{1y}^2+k_{1z}^2)\right\}\right]\exp\left\{-\frac{\alpha_T^2}{8\lambda}\left[(k_{1y}+k_{2x})^2+(k_{1y}+k_{2y})^2\right]\right.$$

$$\left.-\frac{\alpha_T^2}{4}\left[k_{1z}+k_{2z}-\frac{\omega}{v}\right]^2\right\}\exp\left\{-\frac{\alpha_p^2\,\omega^2}{4\gamma^2 v^2}\right\} \qquad (9)$$

where

$$B = \frac{4\pi^{7/2}}{\hbar v}\,N\,\frac{V_0}{\lambda}\,a^2\sqrt{R_p R_T}\,R_T\,r_c^3\exp\left\{\frac{R_p}{2a}\right\}$$

$$\lambda = \frac{1}{2}\left\{1+\frac{R_T}{R_p}\right\} .$$

The total cross section due solely to the strong interaction can be obtained as

$$\sigma_s = 2\pi\int_{R_p+R_T}^{\infty} db\, b\,\frac{A_T^2}{2}\,|a_s(b)|^2$$

$$= \frac{16\pi^8}{\hbar^2 v^2}\,\frac{N^2V_0^2}{\lambda^2}\,A_T^2\,a^5(R_pR_T)\,R_T^2(R_p+R_T)\,r_c^6\exp\left\{\frac{R_p-R_T}{2a}\right\}$$

$$\times\left[\exp\left\{-\frac{r_c^2}{4}k_2^2\right\}+\exp\left\{-\frac{r_c^2}{4}k_1^2\right\}\right]^2\exp\left\{-\frac{\alpha_T^2}{4\lambda}\left[(k_{1x}+k_{2x})^2+(k_{1y}+k_{2y})^2\right]\right.$$

$$\left.-\frac{\alpha_T^2}{2}\left[k_{1z}+k_{2z}-\frac{\omega}{v}\right]^2\right\}\exp\left\{-\frac{2aR_p\omega^2}{\gamma^2 v^2}\right\} . \qquad (10)$$

We see that all the energy dependence (through the γ factor) is contained in the last term while the mass number dependence comes out through the radius R_p and R_T (R_p, $R_T \sim A^{1/3}$).

2c. THE COULOMB PART OF THE AMPLITUDE a_{c_1}

In this section we present the derivation of an analytical expression for a_c. We show all essential steps and necessary approximations in order to obtain such result. The approximations were used due to the fact that in this case we do not only have to deal with gaussians. Numerical tests confirmed the accurateness of the necessary approximations and we are confident in the analytical results which follow. As we shall see they allow for a physically transparent comparison with the results of the previous section.

As before we write

$$a_{c_1} = \frac{1}{i\hbar}\int_{-\infty}^{+\infty} dt\, e^{i\omega t}\int d^3r_1 \int d^3r_2\, e^{-i\vec{k}_1\vec{r}_1 - i\vec{k}_2\vec{r}_2}\,\frac{Z_p\, e\, \gamma}{\sqrt{(x_1-X)^2+(y_1-Y)^2+\gamma^2(z_1-vt)^2}}$$

$$\times N \exp\left\{-\frac{(r_1^2+r_2^2)}{2\alpha_T^2}\right\}\left[1-\exp\left\{-\frac{(\vec{r}_1-\vec{r}_2)^2}{r_c^2}\right\}\right] . \qquad (11)$$

The integration over time gives

$$\int_{-\infty}^{+\infty} dt \frac{e^{i\omega t}}{\sqrt{(x_1-X)^2+(y_1-Y)^2+\gamma^2(z_1-vt)^2}} = \frac{2}{\gamma v}\, e^{i\frac{\omega}{v}z_1}\, K_0\left[\frac{\omega}{\gamma v}\sqrt{(x_1-X)^2+(y_1-Y)^2}\right] \qquad (12)$$

and hence

$$a_{c_1} = \frac{1}{i\hbar v}\, 2 Z_p e N \int dx_1 \int dx_2 \int dy_1 \int dy_2 \int dz_1 \int dz_2$$

$$\times \exp\left[-i\left[k_{1x}x_1 + k_{1y}y_1 + \left[k_{1z}-\frac{\omega}{v}\right]z_1 + k_{2x}x_2 + k_{2y}y_2 + k_{2z}z_2\right]\right]$$

$$\times \exp\left\{-\frac{(x_1^2+y_1^2+z_1^2+x_2^2+y_2^2+z_2^2)}{2\alpha_T^2}\right\}\left[1-\exp\left\{-\frac{(x_1-x_2)^2}{r_c^2}-\frac{(y_1-y_2)^2}{r_c^2}-\frac{(z_1-z_2)^2}{r_c^2}\right\}\right]$$

$$\cdot K_0\left[\frac{\omega}{\gamma v}\sqrt{(x_1-X)^2+(y_1-Y)^2}\right] . \qquad (13)$$

Comparing (13) with (8) one realizes that both amplitudes are very similar, the difference being that in (13) the Bessel function replaces the Gaussian in (8). It is also important to remark that the K_0 has a singularity at the origin, which is not the case of the Gaussian.

Wherever the coordinates x_1 and y_1 are not involved the integrals are just Gaussians and can be performed easily. As we shall be working in the same limit considered in ref. 3 ($r_c^2 \ll \alpha_T^2, \alpha_p^2$), from now on we neglect the first (no-correlation) term inside the brackets. The integral over z_1 and z_2 is

$$I_z = \int dz_1 \int dz_2\, e^{-i(k_{1z}-\frac{\omega}{v})z_1 - ik_{2z}z_2} \exp\left\{-\frac{z_1^2+z_2^2}{2\alpha_T^2}\right\}\exp\left\{-\frac{(z_1^2-2z_1z_2+z_2^2)}{r_c^2}\right\}$$

$$= \pi r_c \alpha_T \exp\left\{-\frac{r_c^2}{4}k_{2z}^2\right\}\exp\left\{-\frac{\alpha_T^2}{4}\left[k_{1z}+k_{2z}-\frac{\omega}{v}\right]^2\right\} .$$

The integrals in x_2 and y_2 are easily performed and we get

$$\int dx_2 \exp\left\{-ik_{2x}x_2 - \left[\frac{1}{2\alpha_T^2}+\frac{1}{r_c^2}\right]x_2^2 + \frac{2x_1}{r_c^2}x_2\right\} = \sqrt{\pi}\, r_c \exp\left\{\frac{r_c^2}{4}\left[i\,k_{2x}-\frac{2x_1}{r_c^2}\right]^2\right\}$$

$$\int dy_2 \exp\left\{-i\,k_{2y}y_2 - \left[\frac{1}{2\alpha_T^2}+\frac{1}{r_c^2}\right]y_2^2 + \frac{2y_1}{r_c^2}y_2\right\} = \sqrt{\pi}\, r_c \exp\left\{\frac{r_c^2}{4}\left[i\,k_{2y}-\frac{2y_1}{r_c^2}\right]^2\right\}$$

and the amplitude (13) becomes

$$a_{c_1} = -\frac{2\, Z_p\, e\, N}{i\hbar v}\, I_z\, \pi r_c^2 \exp\left\{-\frac{r_c^2}{4}(k_{2y}^2+k_{2x}^2)\right\}\int dx_1 \int dy_1 \exp\left\{-\frac{1}{\alpha_T^2}(x_1^2+y_1^2)\right.$$

$$\left. - i(k_{1x}+k_{2x})x_1 - i(k_{1y}+k_{2y})y_1\right\} K_0\left\{\frac{\omega}{\gamma v}\sqrt{x_1^2+(y_1-b)^2}\right\} . \qquad (14)$$

Changing variables into polar coordinates the double integral in (14) becomes

$$I = g(b) \int_0^{2\pi} d\theta \int_0^{\infty} dr\, r\, \exp\left\{-\frac{1}{\alpha_T^2}(r^2 + 2\, br\, sen\theta)\right\}$$

$$\times \exp\left\{-i\left[(k_{1x}+k_{2x})\cos\theta + (k_{1y}+k_{2y})\, sen\theta\right] r\right\} K_0\left[\frac{\omega r}{\gamma v}\right] \qquad (15)$$

where

$$g(b) = \exp\left\{-i(k_{1y}+k_{2y})\, b + \frac{1}{\alpha_T^2} b^2\right\} .$$

If we confine ourselves to nucleon emisson along the incident beam axis (as done in ref. 3) the angular integral can be carried out further analytically and one gets

$$I = 2\pi\, g(b) \int_0^{\infty} dr\, r\, \exp\left\{-\frac{1}{\alpha_T^2} r^2\right\} I_0\left[\frac{2br}{\alpha_T^2}\right] K_0\left[\frac{\omega r}{\gamma v}\right] . \qquad (16)$$

We now study in detail what happens to this expression in the limit $r \to 0$. Recalling that $r = \sqrt{x_1^2+(y_1-b)^2}$ this limit corresponds to a situation in which the wave function of nucleon 1 penetrates into the projectile and interacts with its total charge which is concentrated there (at this point the potential has a singularity). This is certainly the most important contribution to the amplitude. Numerical studies strongly suggest the use of asymptotic expressions for I_0 and K_0

$$K_0(x) \cong -\ln(x/2)$$

$$I_0(x) \cong 1 + \frac{x^2}{4} .$$

Integrating (16) we get

$$I = \left\{\pi(\alpha_T^2 + b^2)\ln\left[\frac{2\gamma v}{\alpha_T \omega}\right] + \frac{\pi}{2}\left[\alpha_T^2 C + b^2(C-1)\right]\right\} \exp\left\{-\frac{b^2}{\alpha_T^2}\right\} .$$

The amplitude can finally be written as

$$a_{c_1} = -\frac{2\, Z_p\, e\, N}{i\hbar v} \pi r_c^2 I_z I .$$

We write now a_{c_2} by interchanging everywhere index 1 with index 2 and then write $a_c = a_{c_1} + a_{c_2}$

$$a_c = i\, A\, M_c\, M_z\, I(b)$$

where

$$A = 2\pi^2 \frac{Z_p\, e\, N}{\hbar v} r_c^3 \alpha_T$$

$$M_c = \exp\left\{-\frac{r_c^2}{4} k_{1z}^2\right\} + \exp\left\{-\frac{r_c^2}{4} k_{2z}^2\right\}$$

$$M_z = \exp\left\{-\frac{\alpha_T^2}{4}\left[k_{1z} + k_{2z} - \frac{\omega}{v}\right]^2\right\} .$$

The total (strong + Coulomb) amplitude is the given by eq. (7)

$$a = \frac{Z_T}{\sqrt{2}} a_c - \frac{A_T}{\sqrt{2}} a_s = i\, M_c\, M_z \left[\frac{Z_T}{\sqrt{2}} A\, I(b) - \frac{A_T}{\sqrt{2}} B\, P\, I_s(b) \right]$$

where

$$P = \exp\left\{ - \frac{\alpha_p^2\, \omega^2}{4 \gamma^2 v^2} \right\}$$

$$I_s(b) = \exp\left\{ - \frac{b^2}{4a(R_p+R_T)} \right\} .$$

The cross section can be written as

$$\sigma = 2\pi \int_{R_p+R_T}^{\infty} db\, b\, |a(b)|^2$$

$$= 2\pi M_c^2 M_z^2 \left[\frac{Z_T^2}{2} A^2 I_{Cou} - \frac{Z_T A_T}{2} A\, B\, P\, I_{mix} + \frac{A_T^2}{2} B^2 P^2 I_{strong} \right] . \qquad (17)$$

The first term corresponds to the pure Coulomb term. The second and third terms correspond to the interference and strong interaction terms respectively. They are given by

$$I_{strong} = a(R_p+R_T) \exp\left\{ - \frac{1}{2a} (R_p+R_T) \right\}$$

$$I_{Cou} = \frac{\pi^2}{4} \alpha_T^2 \left\{ \frac{1}{4} \alpha_T^4 \left[C + 2 \ln\left(\frac{2\gamma v}{\alpha_T \omega} \right) \right]^2 + \left[(C-1) + 2 \ln\left(\frac{2\gamma v}{\alpha_T \omega} \right) \right]^2 \right.$$

$$\times \left[\frac{\alpha_T^4}{8} + \frac{\alpha_T^4}{4} (R_p+R_T)^2 + \frac{(R_p+R_T)^4}{4} \right] + \left[C + 2 \ln\left(\frac{2\gamma v}{\alpha_T \omega} \right) \right] \left[(C-1) + 2 \ln\left(\frac{2\gamma v}{\alpha_T \omega} \right) \right]$$

$$\left. \times \left[\frac{\alpha_T^4}{4} + \frac{\alpha_T^2}{2} (R_p+R_T)^2 \right] \right\} \exp\left\{ - \frac{2}{\alpha_T^2} (R_p+R_T)^2 \right\}$$

$$I_{mix} = \frac{\pi}{2\Gamma} \exp\left\{ -\Gamma(R_p+R_T)^2 \right\} \cdot \left\{ \left[C + 2 \ln\left(\frac{2\gamma v}{\alpha_T \omega} \right) \right] + \left[(C-1) + 2 \ln\left(\frac{2\gamma v}{\alpha_T \omega} \right) \right] \right.$$

$$\left. \times \left[\frac{1}{\Gamma} + (R_p+R_T)^2 \right] \right\}$$

where

$$\Gamma = \frac{2R_T + R_p}{4a(R_T+R_p)R_T} \qquad \text{and} \qquad C = 0.577 \ \text{(Euler's constant)} .$$

The cross section for emission of a correlated nucleon pair can be obtained by multiplication of eq. (17) by the density of final plane wave states $d^3k_1 d^3k_2/(2\pi)^6$. In terms of the kinetic energies ε_1 , ε_2 and the directions (θ_1,φ_1), (θ_2,φ_2) of the two nucleons, this cross section is:

$$\frac{d\sigma}{d\varepsilon_1 d\varepsilon_2 d\Omega_1 d\Omega_2} = \frac{2m^3}{(2\pi)^6 \hbar^4} \pi \sqrt{\varepsilon_1 \varepsilon_2}\, M_c^2(\varepsilon_1,\varepsilon_2)\, M_z^2(\varepsilon_1,\theta_1,\varepsilon_2,\theta_2) \left[Z_T^2 A^2 I_{Cou}(\varepsilon_1,\varepsilon_2) \right.$$

$$\left. - Z_T A_T A\, B\, P(\varepsilon_1,\varepsilon_2)\, I_{Mix}(\varepsilon_1,\varepsilon_2) + A_T^2 B^2 P^2(\varepsilon_1,\varepsilon_2)\, I_{strong} \right] . \qquad (18)$$

In the next section we show examples of application of the above formula and compare our results with those previously obtained in ref. 3.

3. NUMERICAL RESULTS

We now consider the application of formula (18) to high energy heavy ion reactions. Nucleon emission will be studied in the $^{40}Ca+^{40}Ca$ system at 14.5 GeV/u and in the

$^{108}Ag+^{235}U$ system at 1 GeV/u. In order to show the competition between the two kinds of interactions involved we shall first consider them separately and then study interference effects. The values of the parameters appearing in eq. (18) are $r_c = 0.7$ fm, $a = 0.65$ fm, $m = 938$ MeV, $r_0 = 1$ fm, $V_0 = 50$ MeV. As already mentioned before only forward–backward emission ($\theta_1 = 0$, $\theta_2 = 180°$) is considered.

In figs. (2–5) the nucleon pair emission cross section is shown. The curves of equal differential cross sections plotted as a function of the final kinetic energies of the two nucleons were calculated using eq. (18).

Figures 2 and 3 illustrate the behaviour of the emission cross section in the $^{40}Ca+^{40}Ca$ system at two different incident energies having $\gamma \cong 14.5$ and $\gamma = 100$ respectively. Both figures show separately the strong (a), Coulomb (b) and strong+Coulomb (c) cross sections. We see that when going from lower (fig. 2) to higher (fig. 3) energies the Coulomb component of total cross section becomes more and more important. Both types of interactions generate curves with the same "sausage like" appearance, the important difference being the position of the peaks (or ridges) which occur at lower nucleon energies in the case of the Coulomb interaction. These interesting features came from the log term ($\ln(2\gamma v/\alpha_T \omega)$) appearing in I_{Cou}, which favours higher incoming energies (actually diverges with the energy) and lower nucleon energies.

Figures 4 and 5 show the same as 2 and 3 for the $^{108}Ag+^{235}U$ system. The bombarding energies are $E_{1ab} \cong 1$ GeV/u (fig. 4) and $E_{1ab} = 100$ GeV/u (fig. 5). Here it is easier to see how an equilibrated mixture (in fig. 4c) goes to a strongly Coulomb dominated mixture (fig. 5c).

4. CONCLUSIONS

In the present paper we discussed in detail the role played by the Coulomb interaction and its relative importance to the strong interaction in what concerns two nucleon emission. The striking differences are essentially two. Regarding the bombarding energy dependence: while the strong interaction exhibits a weak dependence, the Coulomb interaction has a logarithmic dependence (as characteristic of this type of process in general[7]). Furthermore in what concerns the energy of the emitted nucleon, we can also notice that the strong interaction favours higher nucleon kinetic energies than the Coulomb one. This pattern is of course altered if the bombarding energy is increased sufficiently.

Our results suggest that both effects could be seen experimentally and predict the energy range of the nucleon emission which are most favourable for each interaction. It should be very simple to obtain similar results for other combination of target and projectile. The results are almost analytical.

A comparison with experimental data should be very useful not only in verifying our predictions as to the roles played by strong and Coulomb interaction, but to yield information about the correlation length r_c.

The study of long range correlations is also a very interesting research topic and is presently under investigation.

ACKNOWLEDGMENTS

This work was supported in part by FAPESP. We would like to acknowledge C.A. Bertulani, A.F. Toledo Piza and L. Barz for stimulating discussions and W. Pires for giving clever tips for the numerical calculations.

REFERENCES

1. C.A. Bertulani and G. Baur, *Phys. Rep.* **163** (1988) 299.
2. H. Feshbach and M. Zabek, *Ann. Phys.* **107** (1977) 110.
3. C.A. Bertulani et al., *Mod. Phys. Lett.* **14** (1989) 1315.
4. L. Barz and A.F. Toledo Piza, in preparation.
5. P.J. Karol, *Phys. Rev.* **C33** (1975) 1203.
6. L.G. Ferreira Filho, T. Kodama, and M.C. Nemes, *Nucl. Phys.* **A499** (1989) 837.
7. J.D. Jackson, *Classical Electrodynamics*, 2nd Edition, John Wiley and Sons, 1975.

FIGURE CAPTIONS

Fig. 1 — Relativistic collision between a Lorentz contracted nucleus and a nucleon pair in the laboratory frame.

Fig. 2 — Differential cross section eq. (18) as a function of the nucleon kinetic energies $\varepsilon_1, \varepsilon_2$ for the $^{40}Ca+^{40}Ca$ system at $E_{lab} = 14.5$ GeV/u . We present the result obtained in ref. 3 (fig. 2a), the purely Coulomb cross section (fig. 2b) and the sum of both interactions (fig. 2c).

Fig. 3 — The same as fig. 2 at $E_{lab} = 100$ GeV/u .

Fig. 4 — The same as fig. 2 for the $^{108}Ag+^{235}U$ system.

Fig. 5 — The same as fig. 4 at $E_{lab} = 100$ GeV/u .

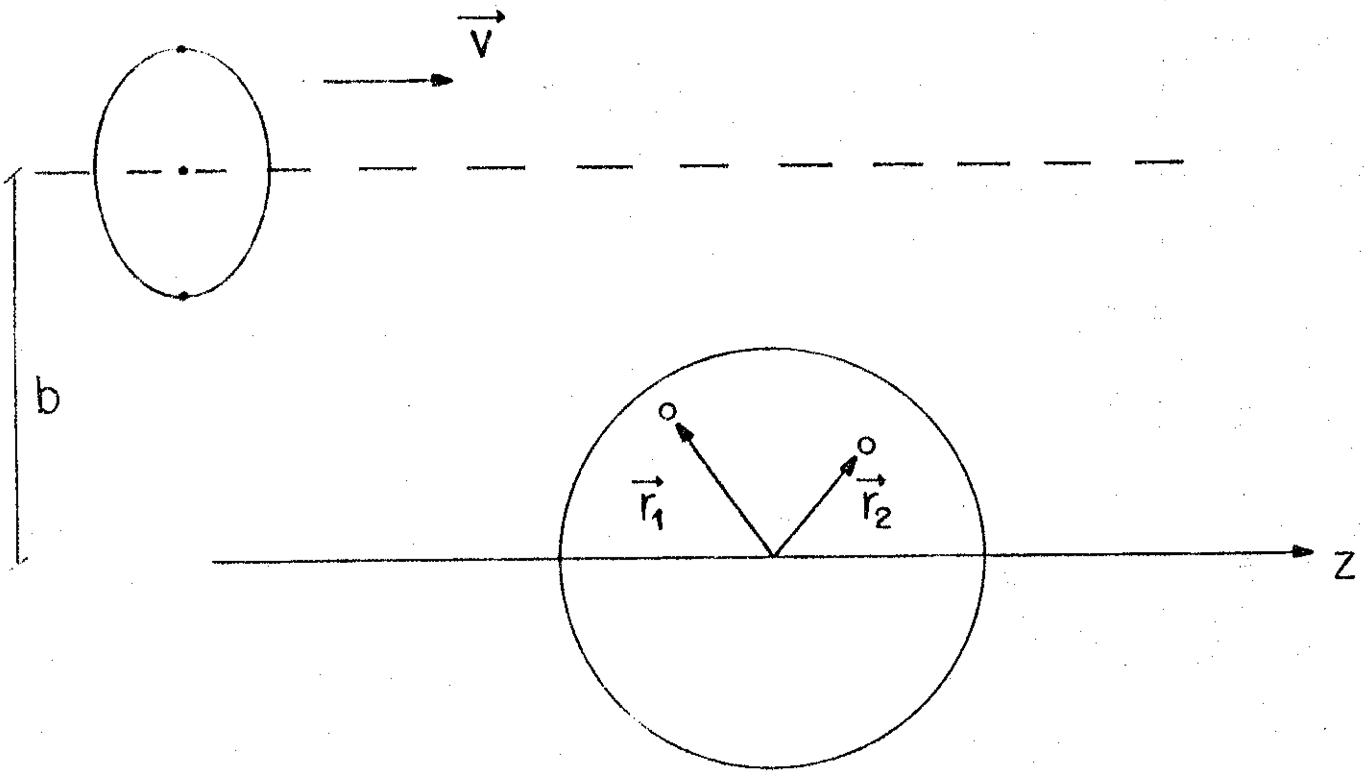

Figure 1

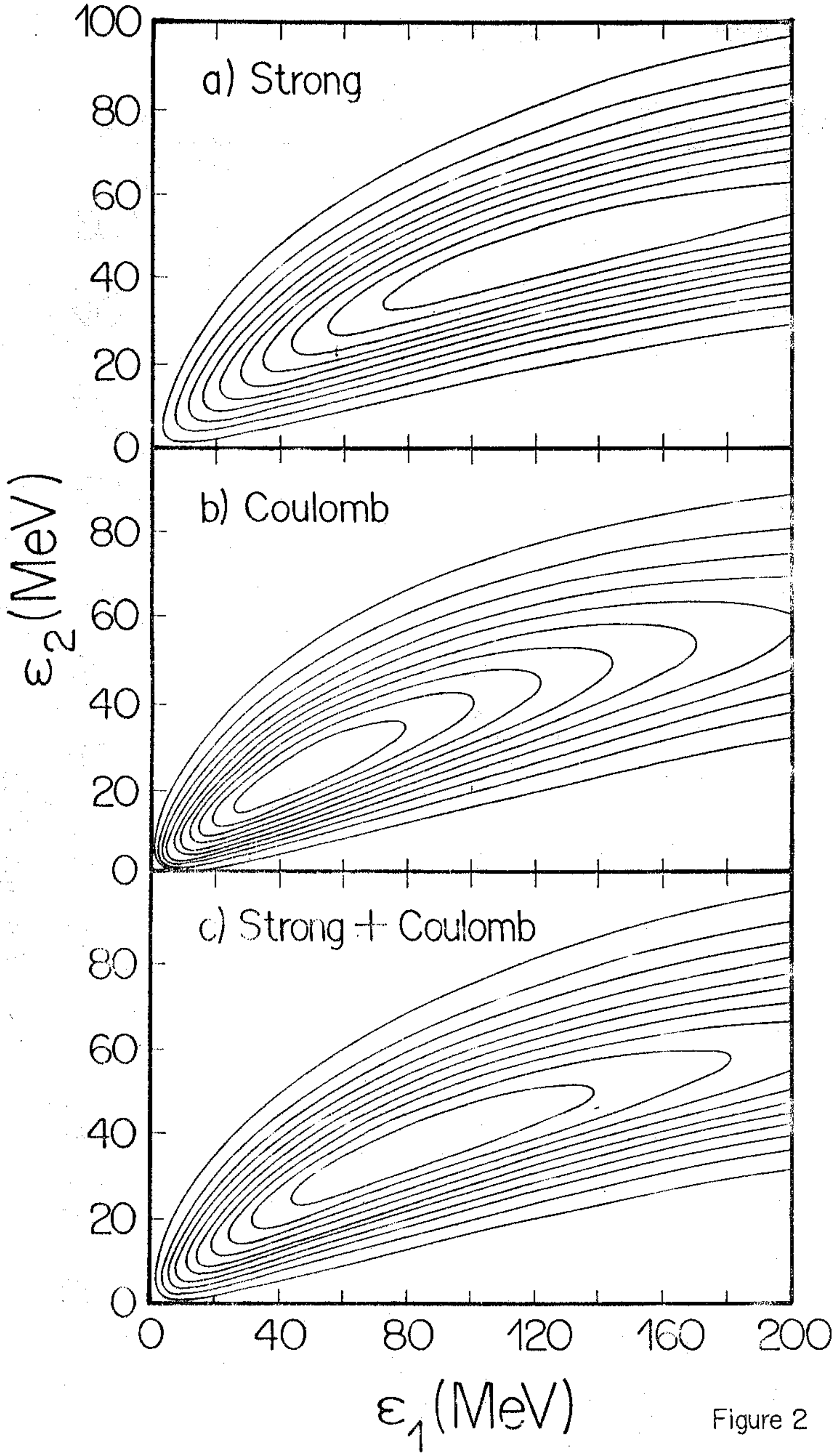

a) Strong
b) Coulomb
c) Strong + Coulomb
100
80
60
40
20
0
0
40
80
120
160
200
ε_2 (MeV)
ε_1 (MeV)

Figure 2

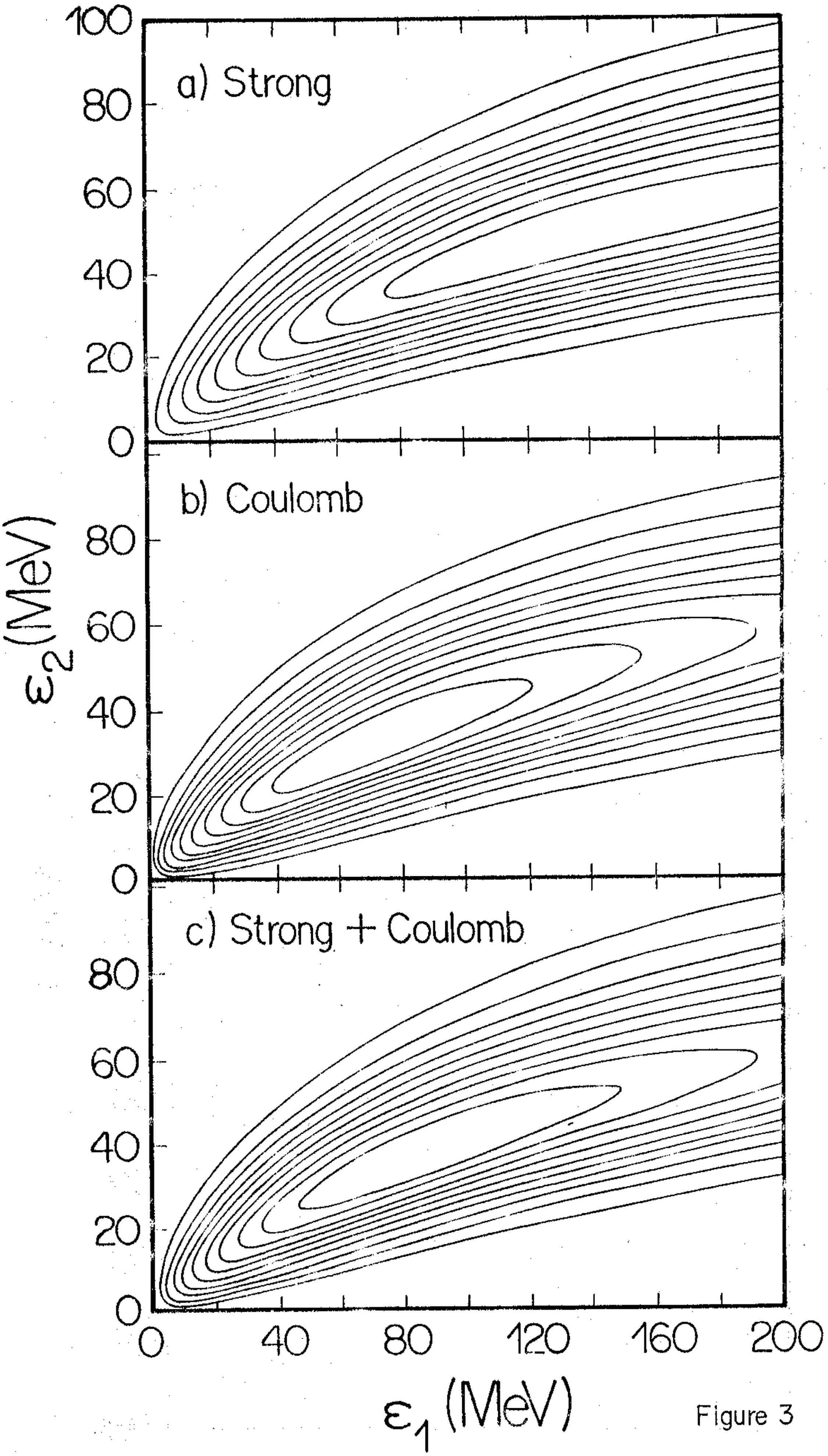
a) Strong
b) Coulomb
c) Strong + Coulomb
ε2 (MeV)
ε1 (MeV)
0
20
40
60
80
100
0
40
80
120
160
200

Figure 3

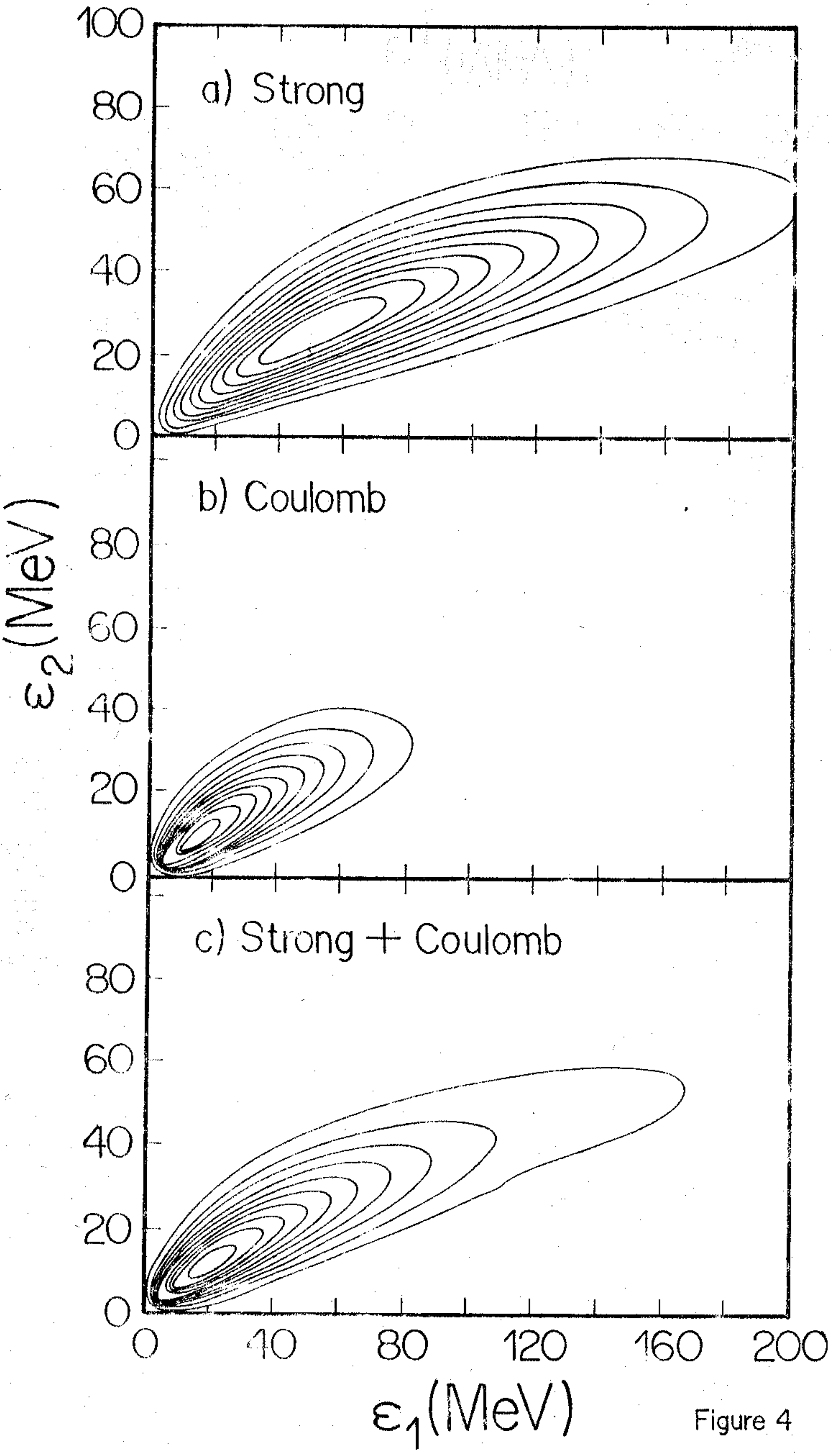
a) Strong
b) Coulomb
c) Strong + Coulomb
ε_2(MeV)
ε_1(MeV)
0
20
40
60
80
100
120
160
200

Figure 4

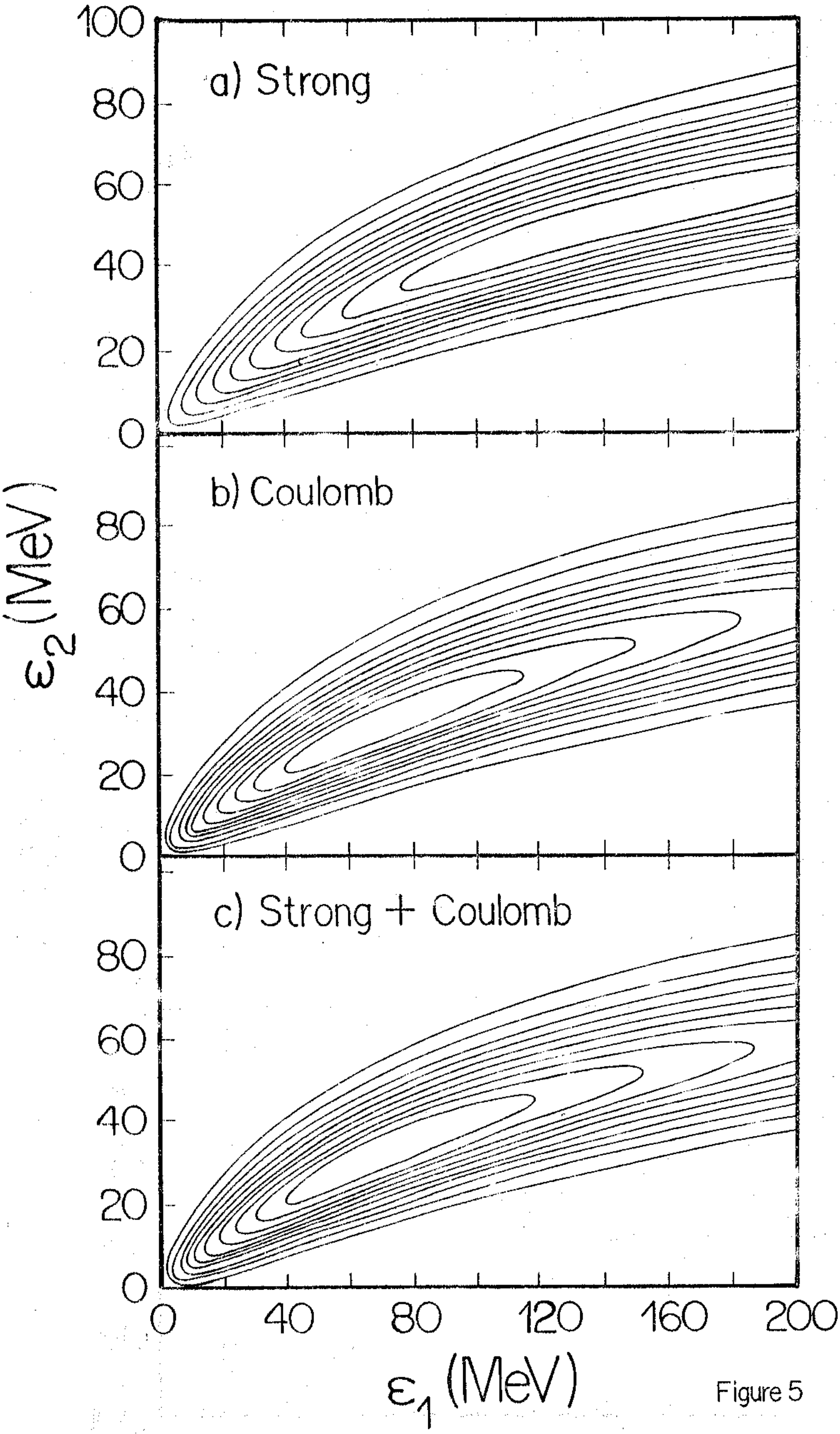
a) Strong
b) Coulomb
c) Strong + Coulomb
100
80
60
40
20
0
ε2 (MeV)
0
40
80
120
160
200
ε1 (MeV)

Figure 5